Size effects on the thermodynamic behavior of a simplified generalized scalar Yukawa model

L. M. Abreu,[1,*] E. S. Nery,[1,†] and A. P. C. Malbouisson[2,‡]

[1]*Instituto de Física, Universidade Federal da Bahia, 40210-340, Salvador-BA, Brazil*

[2]*Centro Brasileiro de Pesquisas Físicas, CBPF/MCTI, 22290-180 Rio de Janeiro, RJ, Brazil*

(Received 14 January 2015; published 16 April 2015)

We analyze the thermodynamic behavior of the generalized scalar Yukawa model, composed of a complex scalar field interacting with scalar and vector fields. Finite-size effects on the phase structure are investigated using methods of quantum field theory on toroidal topologies. We focus on the analysis of the phase structure of this model at effective chemical equilibrium, under change of values of the relevant parameters of the model, looking especially to the influence of the spatial compactification on the phase structure.

DOI: 10.1103/PhysRevD.91.087701 PACS numbers: 11.10.Wx, 13.75.Lb, 14.40.Rt

I. INTRODUCTION AND GENERAL FRAMEWORK

The study of phase diagrams of interacting relativistic systems has been important for the understanding of many physical situations, such as cosmological problems, properties of nuclear matter, the confinemenet/deconfinement phase transition of strongly interacting matter, and the formation of quark-gluon plasma in heavy ions collisions [1,2]. One of the most appropriate frameworks to study these subjects is quantum field theory at finite temperature and density.

An emblematic example is the scalar Yukawa model, which consists of interacting charged and neutral scalar bosons. It is often used as the prototype of more realistic theories in many situations. There are several scenarios in which this model is applied, as follows: nuclear physics and bound states of relativistic n-body systems [3–14]; hadron spectrum [15,16]; the effective interaction of scalar quarks in supersymmetric models [17,18]; phase transitions of relativistic systems under the change of magnitude of the interaction [19]; thermodynamic behavior of relativistic systems in a magnetic background [20].

In the context of scalar Yukawa-like models, we believe that there is still room for investigation of another interesting aspects, such as the analysis of finite-size effects on its phase diagram. It is worth noticing that finite-size effects can be introduced by means of a generalized Matsubara prescription, by compactifying spatial dimensions. A recent account on the subject treating concurrently finite temperature and finite-size effects may be found in Ref. [21]. On general grounds, systems defined on spaces or spacetimes with some of its dimensions compactified are of interest in several branches of physics, such as statistical, condensed-matter, high and low energy physics [22–25].

In this sense, here we intend to study finite-size effects on the phase structure of the generalized scalar Yukawa model, that is, a model with a complex scalar field interacting with scalar and vector fields. We treat jointly spatial compactification and the introduction of finite temperature, using the methods presented in Ref. [21], in such a way that any set of δ dimensions ($\delta \leq D$) of the manifold $\mathbf{R}^D$ can be compactified. Notice that if one of the compactified dimensions is fixed as being the imaginary time, $\delta = d + 1$, with d being the number of compactified spatial dimensions. A possible physical motivation for such a study is the description of a thermal gas of interacting particles, for instance, a system composed of charged mesons interacting with a hadronic medium composed of another kind of light mesons. The motivation lies on the use of effective models for the study of the interacting hadronic matter with interactions of Yukawa type, in which case the charged mesons interact mainly by exchange of σ- (simulating the exchange of two pions) and ω-mesons [20,26]. In this framework, in our approach the complex scalar field would represent the D-meson; the real scalar and vector fields could be interpreted respectively, as the scalar σ-meson (corresponding to a resonance of the $\pi - \pi$ scattering) and as the ω-meson. In this way the mean-field approximation could be associated to a first-order estimate of the thermodynamic properties of a mesonic matter.

II. THE MODEL AND THE FORMALISM

Let us consider a bosonic system interacting with pseudo-Goldstone bosons. We take as our basic objects, a complex scalar field, a real pseudoscalar field and a massive vector field, ϕ, σ e ω^μ, respectively. The Lagrangian density is

$$\mathcal{L} = (\partial_\mu \phi)(\partial^\mu \phi^\dagger) - m_\phi^2 \phi\phi^\dagger + \frac{1}{2}(\partial_\mu \sigma)(\partial^\mu \sigma) - \frac{1}{2} m_\sigma^2 \sigma^2 + g_\sigma \phi\phi^\dagger \sigma - \frac{1}{4} W_{\mu\nu} W^{\mu\nu} + \frac{1}{2} m_\omega^2 \omega_\mu \omega^\mu + g_\omega \omega^\mu j_\mu, \quad (1)$$

*luciano.abreu@ufba.br
†elenilsonnery@hotmail.com
‡adolfo@cbpf.br

where $W^{\mu\nu} = \partial^\mu \omega^\nu - \partial^\nu \omega^\mu$ and $j_\mu = i[(\partial_\mu \phi)\phi^\dagger - \phi(\partial_\mu \phi^\dagger)]$; m_ϕ, m_ω e m_σ are, respectively, the masses of the fields ϕ, ω and σ, whereas g_σ and g_ω are, respectively, the coupling constants for the Yukawa interactions $\phi\phi^\dagger\sigma$ and $\phi\phi^\dagger\omega$. It is worth noticing that by solving equations of motion and current conservation we obtain the condition $\partial_\lambda \omega^\lambda = 0$. The present model can be interpreted as a simplified version of the Walecka model, in which the fermionic field (associated to the nucleons) is replaced by a complex scalar field (represented a mesonic field). Therefore, the Lagrangian of the present paper contains the Yukawa couplings of the complex scalar field (ϕ) with the real scalar (σ) and the vector (ω) fields. The present approach is clearly different from other scenarios, as the quartic self-interaction of the scalar field and fermionic fields. These mentioned models have different interactions not involving other kinds of fields, yielding interpretations different from the ones we get in this paper.

In this context, we search to understand the thermodynamic properties and finite-size effects on the system. The simplest way is to consider the interaction between scalar and vector fields in the mean-field approximation; this means that we will neglect fluctuations of the scalar and vector fields and we will replace the σ and ω fields by its classical counterparts, that is, $\sigma = \langle\sigma\rangle$; $\omega = \langle\omega^0\rangle$. with $\omega^\mu = 0$ for $\mu \neq 0$. This approximation allows one to write the Lagrangian density in Eq. (1) as

$$\mathcal{L} = \phi^\dagger[\partial_\mu\partial^\mu - (m_\phi^2 - g_\sigma\langle\sigma\rangle)]\phi + \frac{1}{2}m_\omega^2\langle\omega^0\rangle - \frac{1}{2}m_\sigma^2\langle\sigma\rangle^2 + g_\omega\langle\omega^0\rangle j_0. \quad (2)$$

It can be seen from equations of motion that, in the mean-field approximation, $\langle\sigma\rangle \propto \rho_s$ and $\langle\omega^0\rangle \propto \rho$, with ρ_s e ρ being number and scalar densities, respectively.

We consider the system defined on a D-dimensional spacetime, at finite temperature T and d compactified spatial dimensions, with $\delta = d + 1 \leq D$. Then the partition function is an integral of the form

$$\int \mathcal{D}\phi^\dagger\mathcal{D}\phi\left[\int_0^\beta d\tau \prod_{i=1}^{d}\int_0^{L_i} dx_i \int d^{D-\delta}\vec{z}(\mathcal{L}_E + \mu j_0)\right], \quad (3)$$

where $\beta = 1/T$, $\{L_i\}$ are the compactification lengths of the spatial coordinates and $\mathcal{L}_E$ is the Lagrangian density given by Eq. (2) in Euclidean space. To study the thermodynamic behavior of the system, we assume that it is in equilibrium at a temperature T and chemical potential (density) μ. Finite-size and temperature effects are taken into account along the lines described in [21]: each spatial coordinate x_i is compactified in a length L_i and, as usual, imaginary time is compactified in a length β. The D-dimensional spacetime is spanned by vectors $\mathbf{u} = (\tau, x_1, x_2, \ldots, x_d, \vec{z})$, where τ is the imaginary time and $(x_1, x_2, \ldots, x_d)$ correspond to the compactified spatial coordinates. The Fourier dual of $\mathbf{u}$ is a D-dimensional vector in momentum space, $\mathbf{q} = (k_\tau, k_{x_1}, \ldots, k_{x_d}, \vec{p})$. We also have a $(D-\delta)$- dimensional vector, $\vec{z}$, with corresponding momentum $\vec{p}$, a $(D-\delta)$- dimensional vector in momentum space. As a consequence, in explicit calculations temperature and finite-size effects are implemented through the following changes in the Feynman rules:

$$\int \frac{dk_\tau}{2\pi} \to \frac{1}{\beta}\sum_{n_\tau=-\infty}^{\infty}, \qquad k_\tau \to \frac{2\pi n_\tau}{\beta} - i\mu, \quad (4)$$

$$\int \frac{dk_{x_i}}{2\pi} \to \frac{1}{L_i}\sum_{n_i=-\infty}^{\infty}, \qquad k_{x_i} \to \frac{2\pi n_i}{L_i}. \quad (5)$$

Then, integrating over the fields ϕ and $\phi^\dagger$ we get from Eq. (3) the grand thermodynamic potential,

$$U(T, \{L_i\}) = \frac{V}{2}[m_\sigma^2\langle\sigma\rangle^2 - m_\omega^2\langle\omega^0\rangle^2] - \frac{VY'(0)}{\beta L_1 \ldots L_d}, \quad (6)$$

where $Y(s)$ is the multiple sum obtained after performing the integration over the $(D-\delta)$-dimensional momentum vector remaining from the replacements in Eqs. (4) and (5):

$$Y(s) = \sum_{l,n_1,\ldots,n_d=-\infty}^{\infty} f(s,d)\left[\left(\frac{2\pi l}{\beta} - \mu_{\text{eff}}\right)^2 + \left(\frac{2\pi n_1}{L_1}\right)^2 + \cdots + \left(\frac{2\pi n_d}{L_d}\right)^2 + p^2 + m_{\text{eff}}^2\right]^{-s+(D-\delta)/2}; \quad (7)$$

with $f(s,d) = [1/(4\pi)^{(D-\delta)/2}]\Gamma(s - \frac{D-\delta}{2})/\Gamma(s)$. $Y'(s)$ stands for the derivative of $Y(s)$ with respect to the argument s. In the above equations V is the volume and m_{eff} and μ_{eff} are respectively the effective mass and the effective chemical potential pertaining to the scalar field ϕ: $m_{\text{eff}}^2 = m_\phi^2 - g_\sigma\langle\sigma\rangle$ and $\mu_{\text{eff}} = \mu - g_\omega\langle\omega^0\rangle$.

The summation in Eq. (7) can be rewritten in terms of Epstein-Hurwitz inhomogeneous *zeta*-functions, which have the following representation, valid in the whole complex ν-plane [27],

$$Z_\delta^{c^2}(\nu,\{a_i\},\{b_i\})$$
$$=\frac{\pi^{\delta/2}}{\sqrt{a_1.....a_\delta}\Gamma(\nu)}\left[\Gamma\left(\nu-\frac{\delta}{2}\right)c^{\delta-2\nu}+2\sum_{i=1}^{\delta}\sum_{n_i=1}^{\infty}\cos(2\pi n_i b_i)\left(\frac{\pi n_i}{\sqrt{a_i}c}\right)^{\nu-\frac{\delta}{2}}K_{\nu-\frac{\delta}{2}}\left(\frac{2\pi c n_i}{\sqrt{a_i}}\right)\right.$$
$$\left.+\cdots+2^\delta\sum_{n_1,\ldots,n_\delta=1}^{\infty}\cos(2\pi n_1 b_1).....\cos(2\pi n_\delta b_\delta)\cdot\left(\frac{\pi}{c^2}\sqrt{\frac{n_1^2}{a_1}+\cdots+\frac{n_\delta^2}{a_\delta}}\right)^{(\nu-\frac{\delta}{2})}K_{\nu-\frac{\delta}{2}}\left(2\pi c\sqrt{\frac{n_1^2}{a_1}+\cdots+\frac{n_\delta^2}{a_\delta}}\right)\right], \quad (8)$$

where K_ν is the modified Bessel function of the second kind. We take $D=4$. Notice that $\nu=s-(D-\delta)/2$ and so, the label of the Bessel functions in Eq. (8), $\nu-\delta/2$, does not depend on $\delta=d+1$: $\nu-\delta/2=s-D/2$. This gives K_{s-2} in all cases for D = 4. We will restrict ourselves to $d=1$. In this case, we have the system in equilibrium at a temperature β^{-1} contained inside a reservoir with the form of an infinite hollow slab of thickness $L_1=L$, corresponding to compactification of just one spatial coordinate. We introduce the notations $a_1=(2\pi/\beta)^2$, $a_2=(2\pi/L)^2$, $b_1=-i\mu_{\rm eff}\beta/2\pi$, $b_2=0$.

In order to obtain the thermodynamic potential we must perform in Eq. (6) the derivative of $Y(s)$ with respect to s, for $s\to 0$. This calculation is simplified when related to a result that involves *Gamma*-functions: for any regular function $F(s)$, we have, $\lim_{s\to 0}(d/ds)[F(s)/\Gamma(s)]=F(0)$.

The first term of Eq. (8) is singular as $s\to 0$; however a process of regularization prevents divergence, after subtraction of a pole term: in fact we have that as $s\to 0$, $\Gamma(s-2)\to 1/2s+(3/4+\gamma/2)+\mathcal{O}(s)$, which, by subtracting $1/2s$ leaves a finite quantity. The second term can be arranged as indicated in the preceding relation involving *Gamma*-functions and using the symmetry property of Bessel functions, $K_\nu(z)=K_{-\nu}(z)$. Remembering Eq. (6) for $D=4$ and $d=1$, we get

$$U(m_{\rm eff},T,\mu_{\rm eff},L)=\frac{V}{2}[m_\sigma^2\langle\sigma\rangle^2+U_{vac}-m_\omega^2\langle\omega^0\rangle^2]+\frac{V}{(2\pi)^2}\left[\sum_{n=1}^{\infty}\cosh(n\beta\mu_{\rm eff})\left(\frac{m_{\rm eff}}{n\beta}\right)^2K_2(m_{\rm eff}n\beta)\right.$$
$$\left.\times\sum_{n=1}^{\infty}\left(\frac{m_{\rm eff}}{nL}\right)^2K_2(m_{\rm eff}nL)+2\sum_{n_1,n_2=1}^{\infty}\cosh(n_2\beta\mu_{\rm eff})\left(\frac{m_{\rm eff}}{\sqrt{L^2n_1^2+\beta^2n_2^2}}\right)^2K_2\left(m_{\rm eff}\sqrt{L^2n_1^2+\beta^2n_2^2}\right)\right], \quad (9)$$

where U_{vac} is the (T,μ) independent vacuum contribution coming from the first term in the right-hand side of Eq. (8), and carries the ultraviolet divergences present in the model. As discussed in Ref. [20], we will omit this term henceforth, which can be interpreted as a renormalization by minimal subtraction.

In order to study the thermodynamic behavior of the system, we need to consider separately the state equations for the two sectors of the model,

$$\frac{\partial U}{\partial\langle\sigma\rangle}=0, \qquad \frac{\partial U}{\partial\langle\omega^0\rangle}=0. \quad (10)$$

The solutions of these equations give the values $\langle\sigma\rangle$ and $\langle\omega^0\rangle$ corresponding to the extrema of the grand thermodynamic potential U. Replacing Eq. (9) in the above equations allows one to obtain $\langle\sigma\rangle$ and $\langle\omega^0\rangle$ in terms of Bessel functions involving explicitly the physical parameters, β, L, $m_{\rm eff}$, $\mu_{\rm eff}$. Taking the number of ϕ-particles and antiparticles equal, it follows that the effective chemical potential $\mu_{\rm eff}$ vanishes, and the only possible value of $\langle\omega^0\rangle$ is zero, as remarked in Ref. [20]. Henceforth, we work in this situation, i.e., at chemical equilibrium.

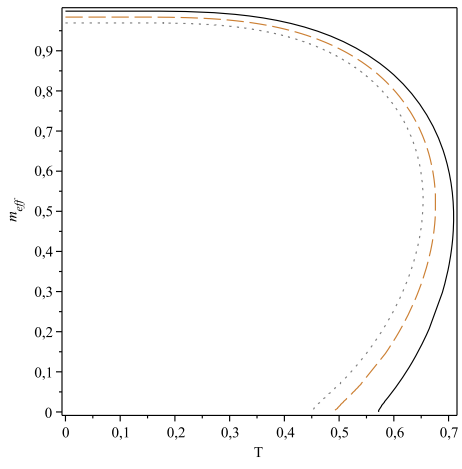

FIG. 1 (color online). Effective mass as a function of temperature, at chemical equilibrium, for $m_\sigma=0.26$ and $g_\sigma=1.52$. Dotted, dashed and full lines represent the system for respectively, $L=2.58$, $L=2.81$ and $L=4.68$.

III. PHASE STRUCTURE AND COMMENTS

Now we are able to perform a qualitative study of the phase structure of the model. In this sense, it is convenient to use the physical quantities in units of the mass of the scalar field ϕ, m_ϕ: $U/m_\phi^4 \to U, m_{\rm eff}/m_\phi \to m_{\rm eff}$, $g_\sigma/m_\sigma \to g_\sigma, T/m_\phi \to T, Lm_\phi \to L$.

Also, in Figs. 2–5 we plot the thermodynamic potential relative to reference state $U(m_{\rm eff}=0)$:

$$\bar{U}(m_{\rm eff},T,L) = U(m_{\rm eff},T,L) - U(m_{\rm eff}=0,T,L). \quad (11)$$

This implies in a shift of the curves leading to negative values on some domains of the vertical axis in these figures.

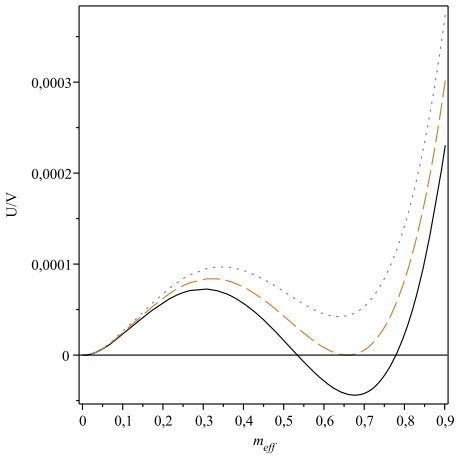

FIG. 2 (color online). Grand thermodynamic potential density $\bar{U}(T,m_{\rm eff})/V$, as a function of the effective mass at chemical equilibrium, for $m_\sigma = 0.26$, $g_\sigma = 1.52$ and $L = 3.74$. Dotted, dashed and full lines represent the isotherms for $T = 0.687$, $T = 0.681$ and $T = 0.677$, respectively.

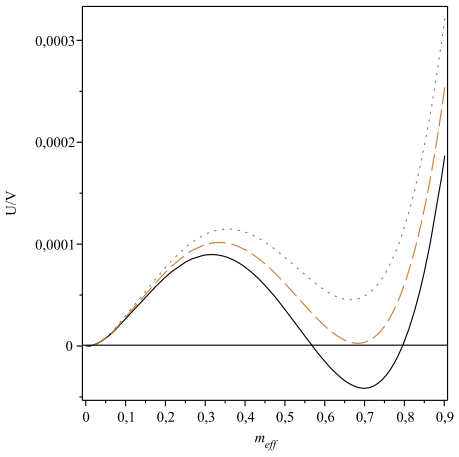

FIG. 3 (color online). Same as in Fig. 2, for $m_\sigma = 0.26$, $g_\sigma = 1.52$ and $L = 2.81$. Dotted, dashed and full lines represent the isotherms for $T = 0.659$, $T = 0.654$ and $T = 0.649$, respectively.

We start by investigating the behavior of the effective mass of the field ϕ in the medium. We plot in Fig. 1 values for $m_{\rm eff}$ that are solutions of the gap equation, as functions of the temperature for different values of the size of the compactified coordinate. It can be seen that the behavior of the effective mass is modified by the presence of the boundary. At zero temperature, the allowed values of $m_{\rm eff}$ slightly decrease as the size of the compactified coordinate is diminished.

In addition, when the dependence of $m_{\rm eff}$ with the temperature is analyzed, we notice its rapid fall to zero at a given temperature, similarly to a liquid-gas first-order phase transition. But the point here is that the curves for $m_{\rm eff}$ corresponding to lower values of L have a faster decrease and fall to zero at smaller values of the

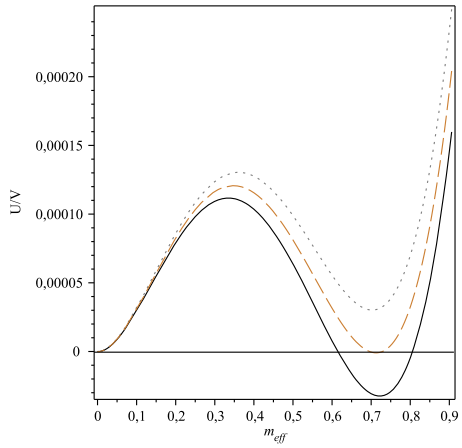

FIG. 4 (color online). Same as in Fig. 2, for $m_\sigma = 0.26$, $g_\sigma = 1.52$ and $L = 1.87$. Dotted, dashed and full lines represent the isotherms with $T = 0.541$, $T = 0.537$ and $T = 0.532$, respectively.

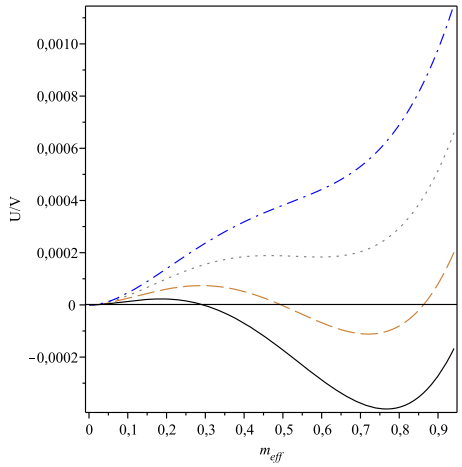

FIG. 5 (color online). Same as in Fig. 2, for $m_\sigma = 0.26$, $g_\sigma = 1.52$ and $T = 0.64$. Dot-dashed, dotted, dashed and full lines represent respectively, the curves with $L = 2.06$, $L = 2.34$, $L = 2.80$ and $L = 3.74$.

temperature. Thus, we can infer that one of the consequences of the presence of boundaries is to cause the decreasing of the temperature at which m_{eff} vanishes. Moreover this effect appears to be more significative than the differences among the values of m_{eff} at $T = 0$ for different values of L, mentioned above. Also, it can be seen from Fig. 1 that for a same value of the temperature, the corresponding values of m_{eff} are larger for smaller values of the size of the system, L.

In order to have a better understanding of the details of this phase transition, in Figs. 2–4 are plotted the grand thermodynamic normalized potential density as a function of the effective mass for different values of the temperature. Each plot is built at a given value of the size of the compactified coordinate. These plots confirm the first-order nature of the transition for all considered sizes. Also, they show the decreasing of the critical temperature as the size L diminishes. Explicitly, in units of m_ϕ in the figures, we have for $L = 3.74$, $T_c(L = 3.74) = 0.689$, for $L = 2.81$, $T_c(L = 2.81) = 0.654$ and for $L = 1.87$, $T_c(L = 1.87) = 0.537$. Finally, in Fig. 5 is plotted the grand thermodynamic normalized potential density as a function of the effective mass, for different values of L and at a fixed value of temperature. It is seen that, starting from a small enough value of L, the system, at a fixed temperature, is driven from the disordered to the broken phase, as its size grows, in other words, it can be said that the presence of the boundaries tends to inhibit the broken phase.

ACKNOWLEDGMENTS

We thank financial support from CAPES, CNPq and FAPERJ, Brazilian agencies.

[1] M. Le Bellac, *Thermal Field Theory* (Cambridge University Press, Cambridge, England, 1996).
[2] J. I. Kapusta and C. Gale, *Finite Temperature Field Theory: Principles and Applications* (Cambridge University Press, Cambridge, England, 2006).
[3] J. W. Darewych, Can. J. Phys. **76**, 523 (1998).
[4] G. V. Efimov, arXiv:hep-ph/9907483.
[5] B. Ding and J. W. Darewych, J. Phys. G **26**, 907 (2000).
[6] V. Shpytko and J. Darewych, Phys. Rev. D **64**, 045012 (2001).
[7] A. Duviryak and J. W. Darewych, J. Phys. A **37**, 8365 (2004).
[8] K. Barro-Bergflodt, R. Rosenfelder, and M. Stingl, Few-Body Syst. **39**, 193 (2006).
[9] M. Emami-Razavi and M. Kowalski, Phys. Rev. D **76**, 045006 (2007).
[10] M. Emami-Razavi, Phys. Rev. D **77**, 045025 (2008).
[11] M. Emami-Razavi, N. Bergeron, J. W. Darewych, and M. Kowalski, Phys. Rev. D **80**, 085006 (2009).
[12] M. Emami-Razavi, N. Bergeron, and J. W. Darewych, J. Phys. G **37**, 025007 (2010).
[13] M. Emami-Razavi, N. Bergeron, and J. W. Darewych, J. Phys. G **38**, 065004 (2011).
[14] A. Chigodaev and J. W. Darewych, Can. J. Phys. **91**, 279 (2013); **91**, 764 (2013).
[15] G. V. Efimov and G. Ganbold, Phys. Rev. D **65**, 054012 (2002).
[16] G. Ganbold, Phys. Part. Nucl. **43**, 79 (2012).
[17] J. Guasch, S. Peñaranda, and R. Sanchez-Florit, J. High Energy Phys. 04 (2009) 016.
[18] A. Abrahantes, J. Guasch, S. Peñaranda, and R. Sanchez-Florit, Eur. Phys. J. C **73**, 2368 (2013).
[19] V. E. Rochev, J. Phys. A **46**, 185401 (2013).
[20] L. M. Abreu, A. P. C. Malbouisson, J. M. C. Malbouisson, E. S. Nery, and R. Rodrigues da Silva, Nucl. Phys. **B881**, 327 (2014).
[21] F. .C. Khanna, Adolfo P. C. Malbouisson, Jorge M. C. Malbouisson, and A. E. Santana, Phys. Rep. **539**, 135 (2014).
[22] N. Arkani-Hamed, A. G. Cohen, T. Gregoire, E. Katz, A. E. Nelson, and J. G. Walker, J. High Energy Phys. 08 (2002) 021; N. Arkani-Hamed, A. G. Cohen, E. Katz, and A. E. Nelson, J. High Energy Phys. 07 (2002) 034.
[23] N. Arkani-Hamed, A. G. Cohen, and H. Georgi, Phys. Lett. B **513**, 232 (2001).
[24] A. J. Roy and M. Bander, Nucl. Phys. **B811**, 353 (2009).
[25] C. Ccapa Ttira, C. D. Fosco, A. P. C. Malbouisson, and I. Roditi, Phys. Rev. A **81**, 032116 (2010).
[26] Gui-Jun Ding, Phys. Rev. D **79**, 014001 (2009).
[27] E. Elizalde, *Ten Physical Applications of Spectral zeta Function*, Lecture Notes in Physics (Springer-Verlag, Berlin, 1995).